ACS OMEGA

Open Access

http://pubs.acs.org/journal/acsodf

Article

Molecular Simulation of Thermodynamic Properties of CH_4/CO_2 Adsorption by Coal Molecules at Different Temperatures and Moisture Contents under Variable Pressure Conditions

Published as part of ACS Omega virtual special issue "CO2 Geostorage".

Tinggui Jia, Xingyu Wu,* and Guona Qu

Cite This: *ACS Omega* 2023, 8, 48381−48393

Read Online

ACCESS | Metrics & More | Article Recommendations

ABSTRACT: In order to further elucidate the thermodynamic mechanism of CH_4/CO_2 adsorption by coal molecules, the adsorption behavior of a molecular model of coal ($C_{206}H_{128}O_{36}N_2$) at Wucaiwan, Zhundong was investigated by applying Materials Studio 2020 and Monte Carlo (GCMC) simulation methods, and the adsorption behavior of CH_4 and CO_2 was studied from the thermodynamic point of view under the conditions of different temperatures, pressures, and moisture contents. The results showed that at different temperatures or moisture contents, CH_4 molecules had a low-density scattering distribution and CO_2 molecules had a high-density polymerization distribution. Temperature and moisture content and adsorption constants a and b were negatively correlated. Under the same conditions, the relationship between single- and binary-component adsorption amounts was $CO_2 > CH_4$ and the relationship between heat of adsorption was $CO_2 > CH_4$. When adsorption potential energy or entropy of adsorption was the same, the adsorption capacity was $CO_2 > CH_4$. Temperatures and moisture contents were negatively correlated with the total adsorption capacity of CH_4/CO_2; pressure was positively correlated with the total adsorption capacity of CH_4/CO_2. The effect of temperature on the equivalent heat of adsorption was greater than that of pressure at different temperatures, and the entropy of adsorption was positively correlated between temperature and CH_4/CO_2, while the amount of adsorption was negatively correlated with the entropy of adsorption. The effect of moisture content on the equivalent heat of adsorption was greater than that of pressure at different moisture contents, and the entropy of adsorption was negatively correlated between moisture content and amount of adsorption. The adsorption entropy of CH_4/CO_2 was negatively correlated, and the adsorption amount was positively correlated to the adsorption entropy. At a temperature above 318 K or moisture content above 10%, the total CH_4/CO_2 adsorption decreased significantly and the CO_2 adsorption decreased significantly. From a thermodynamic point of view, the presence of a large amount of H_2O had a much greater effect on CO_2 than on CH_4, and an increase in temperature or moisture content was unfavorable for CO_2 sequestration, CO_2 stripping of CH_4, and control of CH_4 diffusion and desorption, whereas at low temperature, high pressure, and moisture content <1%, the effect of stripping, sequestration, and control was good.

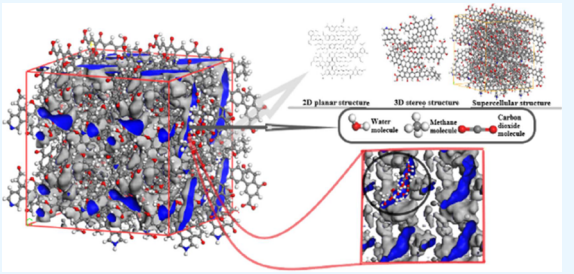

1. INTRODUCTION

Coalbed methane (CBM) has become an important unconventional natural gas resource contributing to global energy stress.[1] As a porous medium, the adsorption capacity of coal for gas is influenced by the pore structure of the coal, ambient temperature, pressure conditions, moisture content, and maturity.[2,3] One of the main challenges in CBM production is that the extraction of gas is accompanied by large amounts of water.[4] A focus on temperature, pressure, and moisture content is inevitable for the production process. Therefore, there is an urgent need to study the variation of these various factors. Injection of CO_2 into unmineable coal seams is considered a promising method for CO_2 sequestration to displace CBM.[5−8] CO_2-ECBM is the injection of CO_2 into coal seams to enhance methane recovery. The technology not only achieves increased production of CBM but also sequesters CO_2 in coal seams and realizes carbon emission reduction. The theoretical basis is the competitive adsorption of CO_2 and CH_4, and the adsorption process is usually accompanied by changes in the thermodynamic properties.[9] At present, many scholars have studied the adsorption characteristics of CH_4 and CO_2 in coal. Bachu et

Received: October 9, 2023
Revised: November 24, 2023
Accepted: November 28, 2023
Published: December 8, 2023

al.[10] demonstrated through theoretical analysis that injecting CO_2 into coal seams can achieve an increase in methane production. Goodman et al.[11] applied adsorption isotherms to characterize the gas storage capacity of coal, which is crucial for the study of CO_2 sequestration technology. Wang et al.[12] investigated the displacement of CH_4 by N_2 and CO_2 through CO_2-ECBM displacement simulation experiments to improve CBM recovery and showed that gas injection significantly improved CBM recovery but CO_2 injection was superior to N_2. Ma et al.[13] demonstrated that the heat of adsorption of CO_2 was much greater than that of CH_4 through adsorption−desorption experiments of CH_4 and CO_2, and that when competing for adsorption, CO_2 dominated. Krooss et al.[14] performed high-pressure adsorption measurements of CH_4 and CO_2 on different grades of dry and moisture equilibrium Pennsylvania coals and showed that the methane adsorption capacity of moisture equilibrium coals was about 20−25% lower than that of dry coals. Day et al.[15] investigated the effect of moisture on 55 bituminous coals in Australia and China and showed that the maximum adsorption capacity of wet coals for CO_2/CH_4 was significantly lower than that of dry coals. Zhou et al.[16] displaced CBM by injecting N_2 and CO_2 into the coal, and CO_2 dominated as CBM increased. Zhang et al.[17] showed that the adsorption capacity of coal samples for CH_4 and CO_2 was significantly stronger than that of CH_4 through the adsorption and transport experiments of coal on CH_4 and CO_2 mixtures. Lun[18] confirmed that the larger the specific surface area of coal, the larger the amount of adsorbed gases, and that the increase in moisture content would reduce the specific surface area of coal through the experiments. Wen et al.[19] experimentally showed that CO_2 injection into coal samples could cause some pores on the coal surface to change from microporous to mesoporous and could effectively promote methane emission from coal seams. Liu et al.[20] demonstrated that CO_2 injection had a positive production effect on the enhancement of CH_4 by using the numerical simulation of CO_2-ECBM.

In addition to the experimental approach, some scholars used molecular simulation methods to carry out the research. Long et al.[21] investigated the adsorption mechanism of multigas systems in coal molecules by using simulation methods of Grand Canonical Monte Carlo (GCMC) and molecular dynamics (MD) methods and demonstrated that the adsorption behavior of single and multigas systems in coal molecules was in accordance with Langmuir's adsorption law. Dang et al.[22] simulated the adsorption pattern of lignite under different conditions. The behavior of lignite coal using the methods of MD, density functional theory (DFT), and GCMC and investigated lignite coal, and the results showed that the electrostatic force of CO_2 was larger than that of CH_4, which was more easily adsorbed in the micropores of the coal. Qu et al.[23] modeled the molecular structure of anthracite coal and simulated the adsorption characteristics of CH_4/CO_2 gases using the GCMC method and found that the CO_2 molecules with stronger adsorption capacity would displace the CH_4 molecules with weaker adsorption capacity from the surface of the coal body. Xiang et al.[24] used the GCMC and MD methods to simulate the adsorption behavior of CH_4/CO_2/N_2 in the coal body, and the results showed that the coal−CH_4 interaction was physisorption, and the coal−CO_2 interaction was mainly a combination of physical adsorption and weak chemical adsorption. Jia et al.[25] constructed a molecular model by using the MS software and found that the oxygen-containing functional groups favored CO_2 adsorption, and the aliphatic functional groups favored CH_4 and N_2 adsorption. Hao et al.[26] showed that the increase of internal moisture of coal decreases the CH_4 adsorption performance by molecular simulation. Zhang et al.[27] explained the methane adsorption mechanism of coal and indicated that the change of methane adsorption is due to the change of free energy of coal surface. Jia et al.[28] used experimental and GCMC methods to analyze the adsorption of gas molecules on the coal surface from a microscopic point of view, and the competitive adsorption of gases on the surface of coal macromolecules was ranked as follows: H_2O > CO_2 > N_2 > O_2 > CH_4 > CO. Zhang et al.[29] showed that by constructing a model of bituminous, coking and anthracite coals, the adsorption of CH_4 follows the order of bituminous coals > anthracite > coking coals, and the presence of water molecules has a limited effect on the heat of adsorption. Gensterblum et al.[30] explained thermodynamically that the mobility of molecules within the adsorbed phase is more restricted when water is preadsorbed. Abunowara et al.[31] confirmed thermodynamically that the adsorption of CO_2 with coal is an exothermic process where CO_2 and water molecules interact with the coal surface under high pressure. Busch[32] pointed out that water adsorption is an important mechanism to control gas adsorption in coal. Li et al.[33] found by molecular simulation that coal with 3% moisture content is favorable for CO_2 displacement of CH_4. Coal with increasing pore size, the selectivity of CO_2 in competitive adsorption decreases, and CO_2 displacement of CH_4 becomes less and less effective.

In terms of CH_4/CO_2 adsorption by coal, the studies are mainly theoretical analysis, adsorption experiments, and molecular simulations. The research purpose is dominated by competitive adsorption, which mainly includes adsorption selectivity, functional group type, pore structure, specific surface area, free energy, and so on. Some scholars have also done related research on the thermodynamic properties of coal adsorption, but there is a lack of fundamental research on the thermodynamic properties of real coal molecules. Therefore, this paper adopts the molecular structure of Jundong Wucaiwan coal to simulate the adsorption behavior of one- and two-component CH_4/CO_2 in coal molecules at different temperatures, pressures, and moisture contents using the GCMC method to explore and analyze the adsorption isotherms, heat of adsorption, potential energy of adsorption, Gibbs free energy, and entropy of adsorption thermodynamic property parameters in the adsorption process. The adsorption behavior of coal macromolecules was analyzed from the thermodynamic point of view to provide certain thermodynamic theoretical basis for CO_2-ECBM technology, the effect of sequestered CO_2 and water on coal adsorption of gas.

2. MODELS AND METHODS

2.1. Coal Molecular Model and Parameters. According to the literature,[34] the author established the structure of Zhundong Wucaiwan coal, the molecular formula of Jundong Wucaiwan coal is $C_{206}H_{128}O_{36}N_2$, and the structure is dominated by aromatic carbon. The carbon mass fraction in the coal is 76.40%, the metamorphic degree is low, and the number of aryl ring condensations is low. The model agrees well with experimental data from industrial and elemental analysis of Jundong coal samples, X-ray photoelectron spectroscopy, X-ray diffraction, Fourier transform infrared spectroscopy, and carbon magnetic resonance spectrometry (^{13}CNMR), and objectively takes into account the sizes of

https://doi.org/10.1021/acsomega.3c07872
ACS Omega 2023, 8, 48381−48393

aromatic nuclei in the metamorphic grade coal, as well as the C, H, O, N surface existence, which can more comprehensively reflect the macromolecular structure of Zhundong high-sodium coal and the related parameters are shown in Table 1.

Table 1. Coal Molecular Structure Modeling Element Mass Fraction

		elemental content(%)			
molecular formula	molecular weight	C	H	O	N
$C_{206}H_{128}O_{36}N_2$	3204	77.15	4.02	17.96	0.87

Coal molecules were optimized by molecular mechanics and molecular dynamics. Using the Forcite module of MS 2020, with Geometry Optimization selected for the task item, smart selected for the optimization method, COMPASS force field, charge using QEq, Coulomb force calculated using Ewald, and van der Waals force and hydrogen bonding interaction calculated using Atom based. The task item is selected Anneal, the number of annealing cycles is 10, the initial temperature is 300 K, the truncation radius is 12.5 Å, the number of steps is 5000, the *NVT* system is comprehensive, the simulation time is 10 ps, the temperature control method is selected Nose, and the force field settings are the same as above. The AC module is used to add 2 coal molecules to form a 2 × 2 × 2 supercell with a density of 1.25 g/cm^3, and the parameters of the coal macromolecule cell are obtained as $a = b = c = 32.43$ Å, as shown in Figure 1.

2.2. Model Construction for Different Moisture Content. In this paper, the cases with 0, 1, 3, 5, and 10% moisture content of the coal body are considered. In order to construct the same adsorption case as the environment of the real water-containing coal body, it is necessary to put an appropriate amount of water molecules into the simulation system and make the simulation system reach equilibrium before calculating the gas adsorption. Choosing Figure 1c. Coal macromolecule, using dynamic in the Forcite module; the density test was performed, and the results showed that the coal macromolecule model is reasonable and can be used for molecular simulation studies. Using the Forcite coal macromolecule module for energy minimization and annealing optimization, the optimization parameters are the same as above, which results in the formation of pores of different sizes, close to the most realistic state of the coal macromolecule structure.[23] The coal macromolecule adsorbs a quantitative amount of H_2O,[35] which is calculated in eq 1 as follows:

$$W = \frac{M_{H_2O}}{M_{total}} \quad (1)$$

where W is the moisture content, %; M_{H2O} is the molar mass of water, g/mol; and M_{total} is the total molar mass of the model, g/mol.

The 1, 3, 5, and 10% moisture content coal macromolecules were constructed using Locate in Sorption module. The calculated quantities according to eq 1 were 14, 43, 71, and 141 moleculars/u.c. for 1, 3, 5, and 10% coal macromolecules, respectively, as shown in Figure 2.

2.3. Analog Parameter Setting. In this paper, MS and GCMC methods are used to simulate the adsorption of single- and binary-component CH_4/CO_2 in coal macromolecules at different temperatures, pressures, and moisture contents. The simulations were performed using the adsorption isotherm module, the simulation loading equilibrium step is 1×10^5, the total process step is 1×10^6, the calculation method is Metropolis; the force field is selected COMPASS; the charge calculation is selected Charge using QEq; the Coulomb force is calculated by Ewald, the van der Waals interaction and hydrogen bonding interaction is calculated by Atom-based method.[26] The simulated temperatures were 298, 308, and 318 K, and the pressure range was 0−10 MPa with an interval of 1 MPa. For the simulations at different temperatures, the adsorbent was selected to be a coal macromolecule with a moisture content of 3%. For simulations with different moisture content, the temperature was fixed at 318 K and the adsorbents were geometrically optimized CH_4 and CO_2 molecules in equal proportions.

The parameter used in the simulation software was fugacity, and the fugacity−pressure relationship was converted to approximate real data. The Soave−Redlich−Kwong (S−R−K) eq of state was introduced,[18,33] especially when equal proportions of CH_4/CO_2 binary-components injection, the S−R−K eq 2 can be used to control the injection of CH_4/CO_2 into the coal body in equal proportions through the S−R−K equation as follows:

$$p = \frac{RT}{V_m - b} - \frac{a\alpha(T)}{V_m(V_m + b)} \quad (2)$$

where $a = \frac{0.45724R^2T_c^2}{p_c}$, $b = \frac{0.08664RT_c}{p_c}$, V_m is the molar volume of the gas; T is the temperature, K; T_c is the critical temperature, K; P is the pressure, MPa; $P_c$the critical pressure, MPa; and R is the gas constant, 8.314 J/(mol·K).

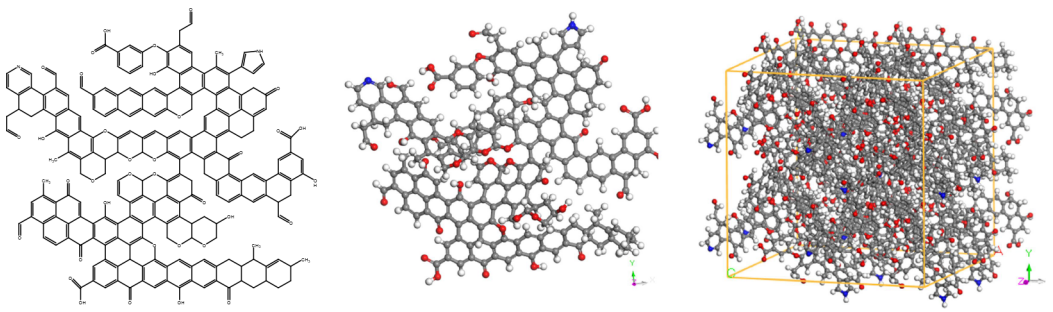

Figure 1. Coal molecular structure: (a) planar structure, (b) 3D stereo structure, and (c) supercellular structure.

https://doi.org/10.1021/acsomega.3c07872
ACS Omega 2023, 8, 48381−48393

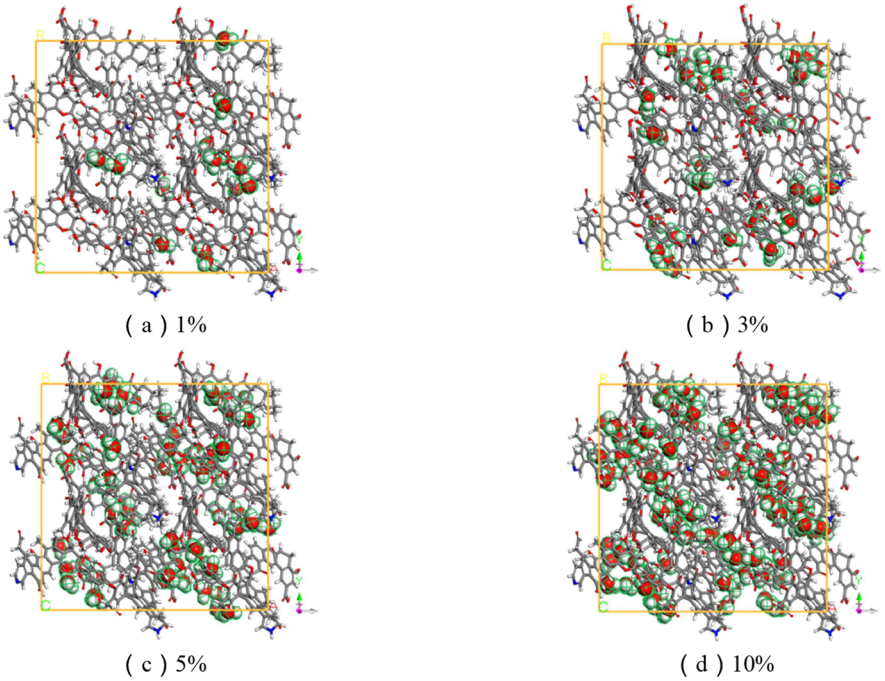

Figure 2. Moisture content of coal macromolecules: (a) 1%, (b), 3% (c) 5%, and (d) 10%.

At the end of the adsorption simulation, the result is obtained as the number of molecules adsorbed, i.e., the number of CH_4/CO_2 molecules adsorbed in each cell in molecular/u.c. The experimentally commonly used adsorption amount is shown in eq 3[18]:

$$V = \frac{N_{am}}{N_a M_s} \times 10^3 \tag{3}$$

where V is the adsorption capacity, mmol/g; N_{am} denotes the number of adsorbed molecules; N_a denotes the number of crystalline cells; M_s is the molecular weight of a single crystalline cell, and N_aM_s is the molecular weight of the skeleton.

2.4. Adsorption Calculator Model. The adsorption model can express the mathematical relationship between the gas adsorption amount and the adsorption conditions, which leads to a better understanding of the microscopic mechanism of CH_4/CO_2 adsorption by coal macromolecules.

The number of adsorbed molecules per unit cell can be obtained by GCMC simulation, and the common adsorption amount can be converted from eq 3. The adsorption process of single- and double-component CH_4/CO_2 adsorption in coal molecules was analyzed using the Langmuir adsorption model, which is the most common model assuming adsorption by monolayer adsorption.[36] The Langmuir model is shown in eq 4

$$V = \frac{abp}{1 + bp} \tag{4}$$

where V is adsorption capacity, mmol/g; a is the saturated adsorption volume, mmol/g; b is the adsorption equilibrium parameter, MPa^{-1}; and p is the pressure, MPa.

Further analysis of the thermodynamic parameters of the CH_4/CO_2 adsorption process in coal molecules, such as the adsorption thermodynamic parameters heat of adsorption Q_{st}, enthalpy change ΔH, Gibbs free energy ΔG, potential energy of adsorption E and entropy change ΔS_n, can directly reflect the interaction between adsorbent and adsorbent molecules.[37−39]

The heat of adsorption can accurately represent the physical or chemical nature of the adsorption phenomenon as well as the activity of the adsorbent, and the equivalent heat of adsorption in the adsorption process can be calculated by using the Clausius−Clapeyron equation. The heat of adsorption is generated because the adsorbent jumps from the position of the higher energy level to the position of the lower energy level during the adsorption process, which leads to an energy transition within the system and manifests as the release of heat from the outside. This leads to an energy transition within the system and manifests itself in the release of external heat.[13,40] The unit of heat of adsorption obtained using the GCMC simulation method is kcal/mol, which must be multiplied by 4.186 to convert to kJ/mol.

Polanyi[41] proposed the theory of adsorption potential energy, which suggests the existence of an adsorption potential field around a solid, in which gas molecules are adsorbed by attractive forces, and gas molecules leave the adsorption potential field and are bound, establishing the relationship between adsorption potential energy, E, and pressure, eq 5, as follows:

$$E = \int_p^{P_0} \cdot \frac{RT}{p} \mathrm{d}p = RT \ln\left(\frac{p_0}{p}\right) \tag{5}$$

where E is the adsorption potential energy, J/mol; R is the universal gas constant, 8.314 J/(mol·K); P is the pressure, MPa; P_0 is the saturated vapor pressure at temperature T, MPa; T is the temperature, K.

The adsorption potential energy can be expressed as a measure of the energy required for a gas to leave the surface of a coal molecule, and the adsorption potential energy, E, can be defined based on the loss of the Gibbs free energy, ΔG, $E = -\Delta G$, as expressed in eq 6[42,43,44]:

https://doi.org/10.1021/acsomega.3c07872
ACS Omega 2023, 8, 48381−48393

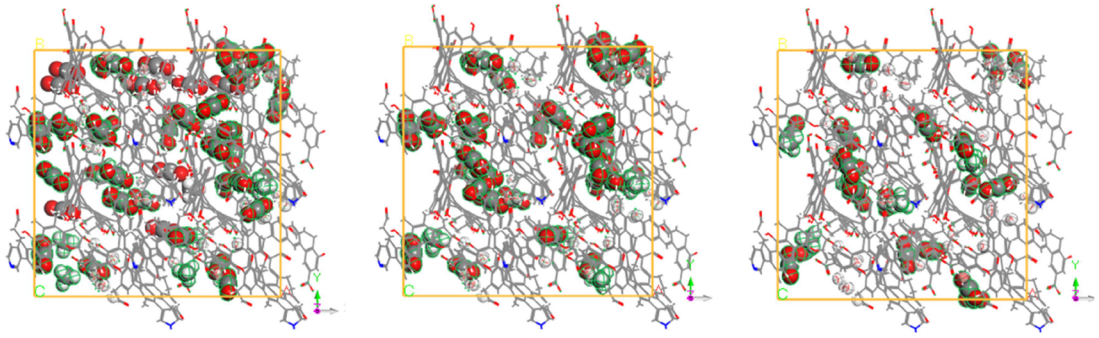

Figure 3. Cellular configurations of binary CH_4/CO_2 at different temperatures: (a) 298 K, (b) 308 K, and (c) 318 K.

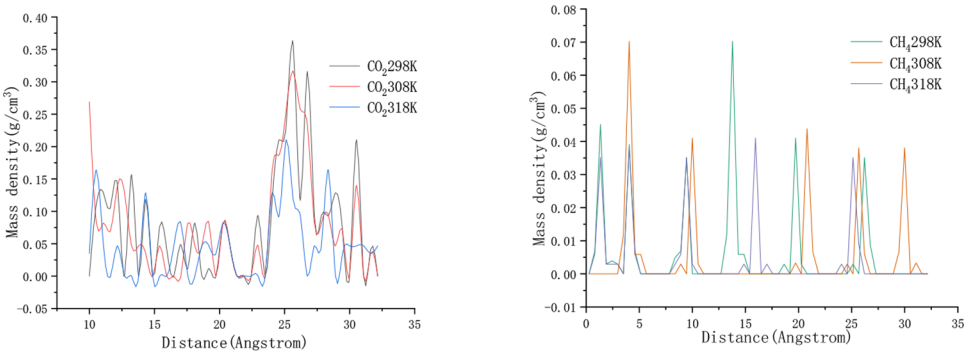

Figure 4. Mass density distribution of binary-component: (a) CO_2 and (b) CH_4 at different temperatures (1 0 0 cross section).

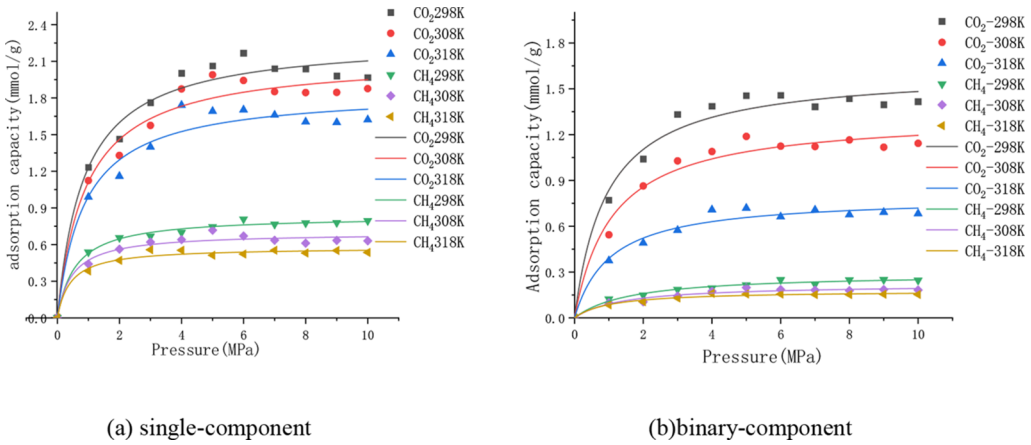

Figure 5. CH_4/CO_2 isothermal adsorption curves at different temperature: (a) single-component and (b) binary-component.

$$\Delta G = -\int_{p}^{p_0} \cdot \frac{RT}{p} \mathrm{d}p = -RT \ln\left(\frac{p_0}{p}\right) \tag{6}$$

where ΔG is the Gibbs free energy, J/mol; R is the gas constant, 8.314 J/(mol·K); P is the pressure, MPa; P_0 is the saturated vapor pressure at temperature T, MPa; and T is the temperature, K.

Dubinin[44] proposed the virtual saturated vapor pressure by statistically analyzing a large number of adsorption test data with the empirical experimental eq 7 to calculate P_0:

$$P_0 = P_c(T/T_c)^2 \tag{7}$$

where P_c is the critical pressure, MPa; T_c is the critical temperature of adsorbate molecules, K. CH_4: P_c = 4.60 MPa and T_c = 190.38 K, CO_2: P_c = 7.38 MPa and T_c = 303.98 K.[31]

The enthalpy change ΔH can be expressed as the energy change of the adsorption process as shown in eq 8[45,46]:

$$\Delta H = -Q_{st} \tag{8}$$

where Q_{st} is the heat of adsorption, kJ/mol.

The entropy of adsorption can measure the degree of chaos in the coal macromolecule adsorption gas system, when coal molecules adsorb CH_4/CO_2 and undergo physical adsorption, the degree of freedom of activity of the gas molecules decreases, and therefore the system $\Delta S < 0$. According to the

https://doi.org/10.1021/acsomega.3c07872
ACS Omega 2023, 8, 48381−48393

fundamental law of thermodynamics, the entropy of adsorption, ΔS, can be expressed according to the Gibbs–Helmholtz equation[33]:

$$\Delta S = (\Delta H - \Delta G)/T \quad (9)$$

where ΔS is the adsorption entropy change, ΔH enthalpy change, and ΔG Gibbs free energy.

3. RESULTS AND DISCUSSION

3.1. Results and Discussion of Different Temperature Conditions.

3.1.1. Adsorption Isotherm Characterization. The cell configurations and mass density distributions of coal molecules with 3% moisture content adsorbing two-component CH_4/CO_2 at 298, 308, and 318 K at a pressure of 10 MPa are shown in Figures 3 and 4. The Langmuir adsorption theory model using eq 4 was fitted to the data obtained from the simulations to obtain the adsorption isothermal curves of CH_4/CO_2 at different temperatures and pressures as shown in Figure 5. The fitting using eq 4 to obtain the fitted parameters of the Langmuir equation at different temperatures is shown in Tables 2 and 3.

Table 2. Single-Component Adsorption Isothermal Curves Langmuir Fitting Coefficients

	a (mmol/g)		b (1/MPa)		R^2	
temperature (K)	CH_4	CO_2	CH_4	CO_2	CH_4	CO_2
298	0.81	2.17	1.70	2.60	0.98	0.98
308	0.71	1.99	2.86	1.78	0.97	0.99
318	0.56	1.74	1.77	2.35	0.99	0.97

Table 3. Binary-Component Adsorption Isothermal Curves Langmuir Fitting Coefficients

	a (mmol/g)		b (1/MPa)		R^2	
temperature (K)	CH_4	CO_2	CH_4	CO_2	CH_4	CO_2
298	0.25	1.46	11.51	2.82	0.98	0.98
308	0.19	1.19	9.54	1.49	0.98	0.99
318	0.16	0.72	1.76	1.34	0.97	0.97

From Figures 3 and 4, it can be seen that the number of both molecules decreases at 298–318 K. Among the coal molecules, CH_4 molecules were distributed in low-density scattering and CO_2 molecules were distributed in high-density aggregation in the pores, which confirmed that coal has a complex pore structure with different sizes, in accordance with the study of Sun.[46] Among them, Figure 4 shows that both CH_4/CO_2 values peaked at 298 K (0.039 g/0.36 g·cm^{-3}). However, there are positive and negative values of CO_2 mass density with increasing temperature, and due to its dynamic exchange with the outside of the supercell, CO_2 is present at the boundary line of the cell, while CH_4 is not reflected because the CO_2 adsorption capacity is much larger than that of CH_4.[28] From Figure 5, it can be seen that at a fixed pressure, as the temperature increases, the adsorption of both mono- and bicomponent CH_4/CO_2 decreases, and the pressure required to reach saturation of the carbon molecules decreases, e.g., CO_2 (bicomponent) reaches saturation at 5 MPa at 298 K, while at 4 MPa at 318 K, due to the increased molecular thermal motion as the temperature increases.[45] At a fixed temperature, CH_4 adsorption is more likely to reach saturation adsorption first as the pressure increases. Both increase rapidly and then level off due to the inhomogeneous distribution on the coal surface. As can be seen from Tables 2 and 3, the R^2 is greater than 0.97, which confirms the reliability of the simulated data. Sun et al.[46]investigated the micromechanical study of CH_4/CO_2 adsorption in different grades of coal, which showed that the micropores are the main adsorption sites. Both adsorption constants a and b increased with decreasing temperature, indicating that the interaction between the coal body and the gas molecules was enhanced at 298 K compared to 308 and 318 K. Long[21] verified that the adsorption behavior of the coal molecular multigas system conforms to Langmuir's adsorption law, and the single- and double-component CH_4/CO_2 adsorption behavior in this paper also conforms to Langmuir's adsorption law. The above analysis shows that CH_4/CO_2 will produce competitive adsorption, and CO_2 occupies most of the adsorption sites. With increasing temperature, the adsorption amounts of both decrease in single-component injection. In binary-components injection, CO_2 affects the adsorption sites of CH_4, and the effect of CO_2 replacing CH_4 is weakened again. Therefore, temperature higher than 318 K or pressures lower than 5 MPa are unfavorable for the adsorption of CH_4/CO_2 by coal macromolecules and the expulsion of CH_4 by CO_2.

3.1.2. Thermal Properties of Adsorption. The equivalent heat of adsorption of single- and binary-component CH_4/CO_2 at different temperatures and pressures is shown in Figure 6.

As can be seen from Figure 6, the equivalent heat of adsorption of CO_2 was larger than that of CH_4 when single-component and two-component injections were carried out, and the trend of change of the equivalent heat of adsorption of the two was not obvious at a fixed temperature and with the increase of pressure, but the adsorption amount of single-component and binary-component CH_4/CO_2 was increased, indicating that the adsorption amount of the two was not only affected by the equivalent heat of adsorption but also affected by other factors. The average heat of adsorption of CH_4 at 298/308/318 K was 23.76/23.3/23.21 kJ/mol with a decreasing trend, and the average heat of adsorption of CO_2 was 39.94/39.31/38.95 kJ/mol with a decreasing trend. In the case of two-component injection, the average heat of adsorption of CH_4 at temperature 298/308/318 K was 24.78/24.36/24.03 kJ/mol with a decreasing trend, while the average heat of adsorption of CO_2 was 38.66/38.29/37.74 kJ/mol with a decreasing trend. Coal adsorption of CH_4 is physisorption, and the equivalent heat of adsorption of CO_2 is close to 42 kJ/mol, indicating that CO_2 can be chemisorbed in coal molecules.[31] The above analysis shows that the adsorption capacity of coal molecules for CH_4/CO_2 decreases with increasing temperature, regardless of single- or binary-component injections, and the temperature is higher than 318 K, which is unfavorable for CO_2 to replace CH_4.

3.1.3. Adsorption Potential Characterization. The virtual saturated vapor pressure P_0 of CH_4/CO_2 calculated according to eq 7 is shown in Table 4.

The results of Table 4 were brought into eqs 5 and 6, and the CH_4/CO_2 Gibbs free energy ΔG was calculated as shown in Figure 7.

As can be seen from Table 4 and Figures 5 and 7, where $E = -\Delta G$, when the pressure is fixed, the total CH_4/CO_2 adsorption decreases with increasing temperature and the adsorption potential energy is negatively correlated with the adsorption amount. When the temperature is fixed, the total CH_4/CO_2 adsorption increases with increasing pressure, and the adsorption potential energy is positively and negatively

https://doi.org/10.1021/acsomega.3c07872
ACS Omega 2023, 8, 48381–48393

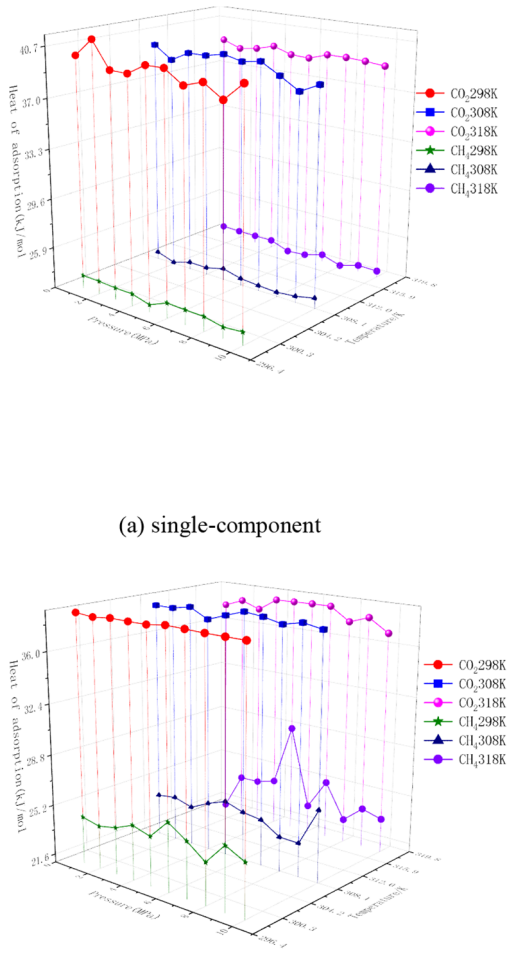

Figure 6. Equivalent heat of adsorption curves: (a) single-component and (b) binary-component.

Table 4. Virtual Saturated Vapor Pressure P_0

temperature/K	CH_4/MPa	CO_2/MPa
298	11.27	7.09
308	12.04	7.58
318	12.83	8.07

correlated to the adsorption amount. Under the same conditions, the adsorption potential energy of CH_4 was smaller than that of CO_2, and the Gibbs free energy of CH_4/CO_2 on the coal body was negative, indicating that spontaneous adsorption of CH_4/CO_2 on the coal body occurred, which belonged to physical adsorption. When $\Delta G > 0$, CO_2 adsorption is still greater than CH_4 adsorption due to the fact that the CO_2 equivalent heat of adsorption is much greater than the CH_4 equivalent heat of adsorption. This results in CO_2 competing for CH_4 adsorption sites when CH_4 adsorption is dominant.[47,48]

3.1.4. Adsorption Entropy Properties. The variation of single-component and binary-component CH_4/CO_2 adsorption versus the adsorption entropy calculated from eq 9 at different temperatures is shown in Figure 8.

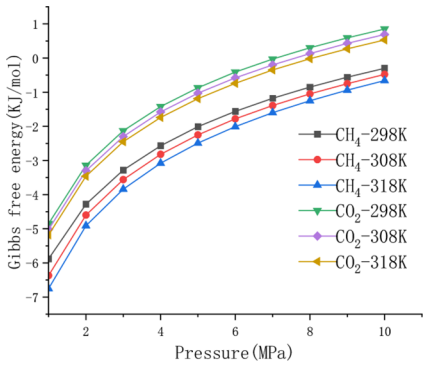

Figure 7. CH_4/CO_2 Gibbs free energy ΔG at different temperature pressures.

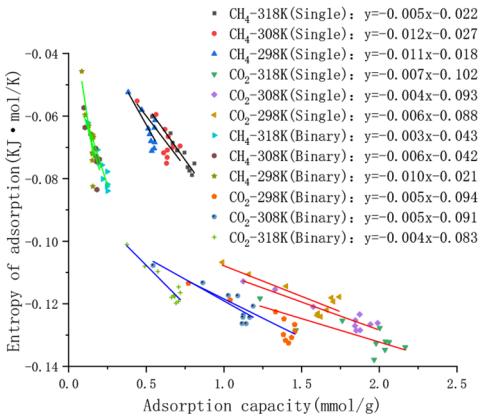

Figure 8. Curve of adsorption amount versus entropy of adsorption at different temperatures.

From Figure 8, it can be seen that the CH_4/CO_2 adsorption is negatively correlated with the adsorption entropy for both single- and dual-component injections. As the temperature increased, the zonal CH_4/CO_2 adsorption entropy increased and more gases were released from the coal surface or pore space, i.e., in the free adsorption state.[49] According to the analysis of the slope of the curve in Figure 8, CO_2 is more affected by temperature than CH_4, CO_2 has a higher replication efficiency at 298 K than at 318 K, and the total adsorption entropy of the binary-component injection is larger than that of the single-component injection, and the fitting coefficient R^2 ranges from 0.98 to 0.78, which suggests that with the increase in temperature, more molecules are in the free state and detached from the pore space. When the adsorption amount is the same, the adsorption entropy of CH_4 is larger than that of CO_2, and when the adsorption entropy is the same, the adsorption amount of CH_4 is smaller than that of CO_2. The above analysis shows that as the temperature increases, the total adsorption entropy increases, the adsorption amount decreases, and more gases are in the free state, which reduces the adsorption capacity of coal on CH_4/CO_2, and the effect is more significant on CO_2.

3.2. Results and Discussion for Different Moisture Content Conditions. *3.2.1. Adsorption Isotherm Characterization.* The cell configurations and mass density distributions of CH_4/CO_2 adsorbed by the two-component adsorbent at different moisture content at a pressure of 10 MPa and a temperature of 318 K are shown in Figures 9 and 10. The adsorption of CH_4/CO_2 at different moisture content is

https://doi.org/10.1021/acsomega.3c07872
ACS Omega 2023, 8, 48381−48393

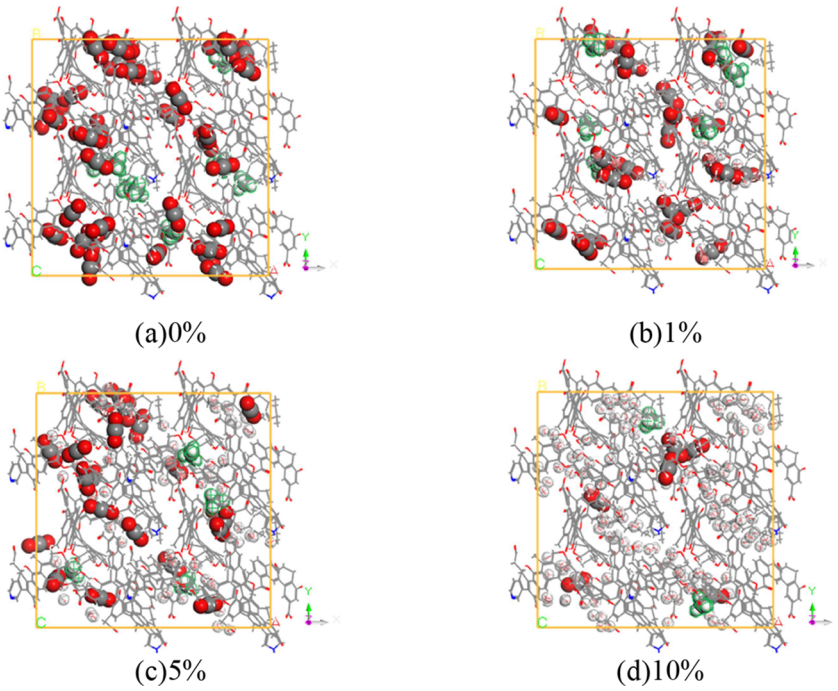

Figure 9. Cellular configurations of binary CH_4/CO_2 at moisture content: (a) 1%, (b) 3%, (c) 5%, and (d) 10%.

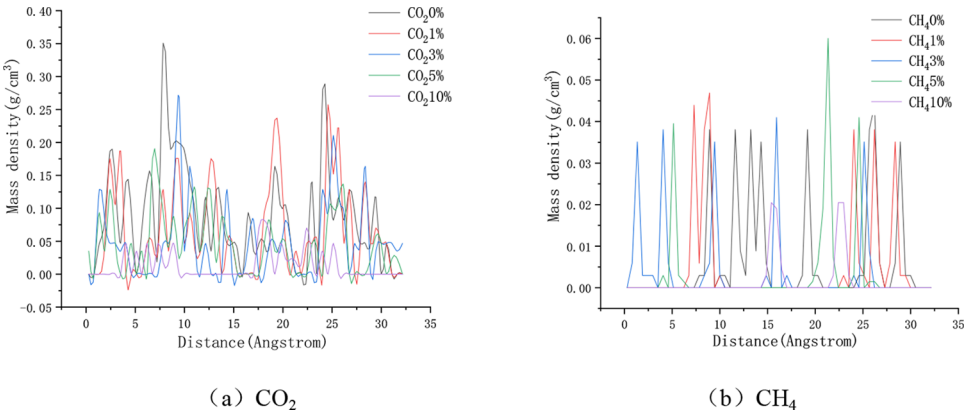

Figure 10. Mass density distribution of binary-component: (a) CO_2 and (b) CH_4 at moisture content (1 0 0 cross section).

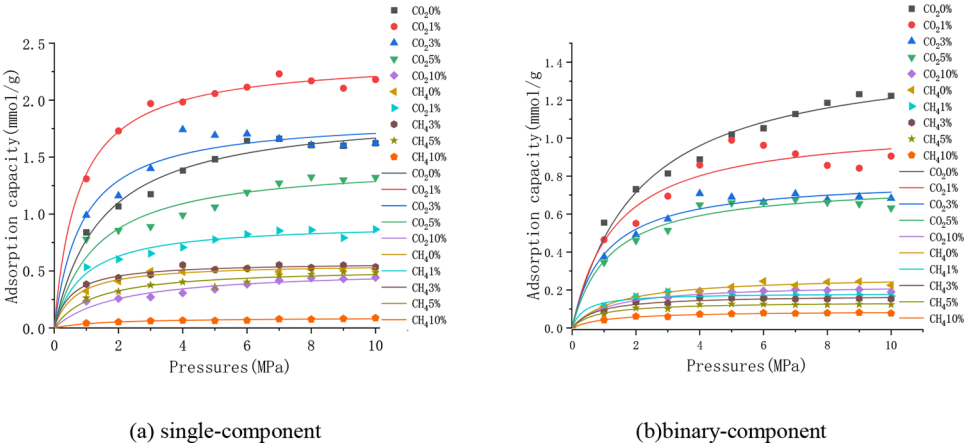

Figure 11. CH_4/CO_2 isothermal adsorption curves at different moisture content: (a) single-component and (b) binary-component.

isothermal. The Langmuir adsorption theory model of eq 4 was used to fit the data to obtain the adsorption isothermal

https://doi.org/10.1021/acsomega.3c07872
ACS Omega 2023, 8, 48381−48393

curves of CH_4/CO_2 at different moisture content and pressures as shown in Figure 11, and the fitting parameters of the Langmuir equation are given in Tables 5 and 6.

Table 5. Single-Component Adsorption Isothermal Curves Langmuir Fitting Coefficients

	a (mmol/g)		b (1/MPa)		R^2	
moisture content (%)	CH_4	CO_2	CH_4	CO_2	CH_4	CO_2
0	0.54	1.65	1.70	2.67	0.98	0.98
1	0.89	2.23	2.86	4.36	0.98	0.99
3	0.56	1.74	1.77	2.35	0.99	0.97
5	0.51	1.42	1.60	1.32	0.96	0.95
10	0.18	0.31	0.55	0.29	0.99	0.98

Table 6. Binary-Component Adsorption Isothermal Curves Langmuir Fitting Coefficients

	a (mmol/g)		b (1/MPa)		R^2	
moisture content (%)	CH_4	CO_2	CH_4	CO_2	CH_4	CO_2
0	0.26	1.25	1.10	4.06	0.98	0.98
1	0.19	1.02	0.83	6.13	0.94	0.93
3	0.16	0.72	1.34	1.76	0.97	0.97
5	0.13	0.68	0.65	1.57	0.98	0.97
10	0.08	0.18	0.37	0.39	0.97	0.95

From Figures 9 and 10, it can be seen that the number of adsorbed molecules decreases for both two-component injections with moisture content from 0 to 10% and that CO_2 is more affected than CH_4, which has a low-density scattering distribution of CH_4 molecules and a high-density aggregation distribution of CO_2 molecules. Among them, Figure 10 shows that there are positive and negative values of CO_2 mass density and the presence of H_2O significantly reduces the adsorption. From Figure 11 and Tables 5 and 6, it can be seen that the one- and two-component CH_4/CO_2 adsorption decreases with an increasing moisture content. At 5−10% moisture content, the CO_2 saturation adsorption amount decreased significantly from (7 MPa) 0.68 to 0.20 mmol/g. While at 1% moisture content, the single-component CH_4/CO_2 saturation adsorption amount both reached peaks at (10 MPa) 0.49 mmol/g and (7 MPa) 2.23 mmol/g, which was attributed to the fact that the liquid water wetted the coal matrix, after which a monomolecular layer of water film was formed on the coal surface, providing more effective adsorption sites.[50] When the moisture content was fixed, the total CH_4/CO_2 adsorption increased with increasing pressure. The CH_4 adsorption increased from 0.54 to 0.89 mmol/g, an increase of 64%, while the CO_2 adsorption increased from 1.65 to 2.23 mmol/g, an increase of 26%. In contrast, with the binary-component injection, the adsorption did not increase significantly as the moisture content increased with a fixed moisture content of 1%. The equilibrium adsorption of CH_4/CO_2 both decreased with increasing moisture content, indicating that water and coal formed part of the chemical water occupying the adsorption sites. The other part of free water filled the pores and covered the surface, thus forming a water film to prevent coal adsorption, which was due to the formation of water clusters between coal molecules and H_2O, which was more easily combined with oxygen-containing functional groups,[51] the adsorption capacity of $H_2O > CO_2 > CH_4$, and the priority order of adsorption was $H_2O > CO_2 > CH_4$. When the moisture content was 10%, the equilibrium adsorption of single-component and double-component CH_4/CO_2 was both drastically. When the moisture content was 10%, the equilibrium adsorption amount of single- and binary-component CH_4/CO_2 was drastically decreased, and the influence of the presence of large amount of H_2O on CO_2 was much larger than that of CH_4. Therefore, when the moisture content was 1%, the injection of a single-component increased the adsorption amount, and in the case of the binary-component, other factors must be taken into account. CO_2 adsorption is negatively correlated with moisture content, whlie the moisture content was higher than 10%, it obviously affected the CO_2 drive CH_4, thus reducing the efficiency of the CO_2 drive CH_4.

3.2.2. Thermal Properties of Adsorption. The heat of adsorption of single-component and binary-component CH_4/CO_2 equivalents at different moisture content and pressures is shown in Figure 12.

As can be seen from Figure 12, both single- and double-component CH_4/CO_2 equivalent heats of adsorption fluctuate slightly with increasing pressure, which is due to the change in pressure, which causes the redistribution of molecules to reach the equilibrium state, resulting in a slight change in the equivalent heat of adsorption. The average heat of adsorption of CH_4 in single-component injection with moisture content of 0−10% was 25.35/23.33/24.01/26.38/25.18 kJ·mol^{-1}, which

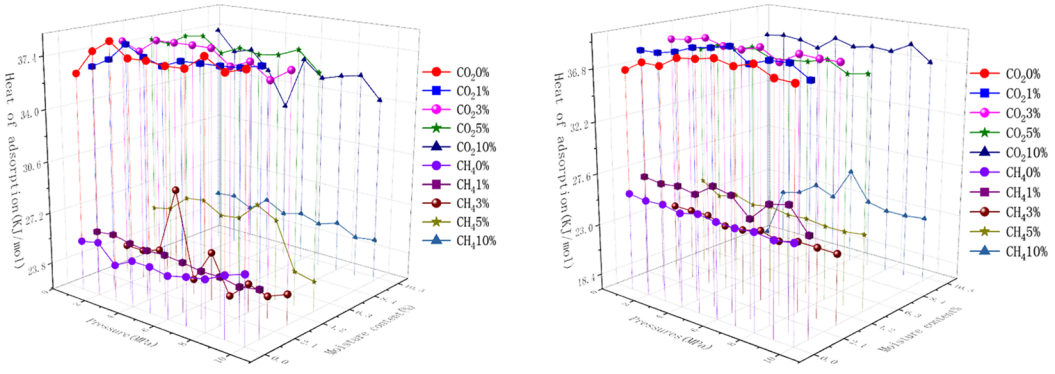

(a) single-component (b) binary-component

Figure 12. Equivalent heat of adsorption curves: (a) single-component and (b) binary-component.

https://doi.org/10.1021/acsomega.3c07872
ACS Omega 2023, 8, 48381−48393

first decreased, then increased, and then decreased again, while the average heat of adsorption of CO_2 was 37.93/37.72/37.78/37.7/35.42 kJ·mol^{-1}, which showed a decreasing trend. The average heat of adsorption of CH_4 injected into the binary-component moisture content from 0 to 10% was 25.62/26.93/23.19/24.02/22.57 kJ·mol^{-1}, with the maximum heat of adsorption at 1% and the overall decreasing trend, while the average heat of adsorption of CO_2 was 38.24/38.80/38.83/37.63/37.50 kJ·mol^{-1}, with a decreasing trend with a slight decreasing trend and the maximum heat of adsorption at 1%. When the moisture content was 10%, the equivalent heat of adsorption of CO_2 was more affected than that of CH_4/CO_2 because with increasing moisture content, there was mainly competition for adsorption space between H_2O/CH_4 and there was competition for adsorption sites and adsorption space between CH_4/CO_2.[52] The analysis showed that the heat of adsorption of CH_4/CO_2 equivalents decreased overall with increasing moisture content, and when the moisture content was higher than 10%, it significantly reduced the efficiency of CO_2 to drive CH_4.

3.2.3. Adsorption Potential Characterization. Calculated according to 4, 5, 6, the curves of CH_4/CO_2 adsorption potential energy versus adsorption amount at different moisture contents are shown in Figure 13.

From Figure 13, it can be seen that in single-component and binary-component injections, with the increase of moisture content, the adsorption potential energy of CH_4/CO_2 is reduced, and CO_2 is more affected by moisture content under the same conditions. Single-component injection, CH_4/CO_2 adsorption potential energy high value in the moisture content of 1%, 10% moisture content adsorption potential energy significantly reduced, this is because a small amount of water clusters can promote the coal adsorption adsorbent.[3] For two-component injection, the adsorption potential energy of CH_4/CO_2 all decreases with the increase of the moisture content in general. According to the curve, R^2 is 0.98−0.95, which indicates that the data are reliable. When the adsorption potential energy is the same, the adsorption amount is CO_2 > CH_4. When the adsorption amount is the same, the adsorption potential energy is CO_2 > CH_4, indicating that the adsorption amount is affected by many factors. Through the single- and binary-component injection data comparative analysis, the effect of H_2O on CO_2 is greater than that on CH_4. In the above analysis, single-component and binary-component injections of coal body, CH_4/CO_2 adsorption potential energy are with the increase of moisture content and decrease, in the moisture content of more than 10% significantly reduced.

3.2.4. Adsorption Entropy Properties. The variation of single- and binary-component CH_4/CO_2 adsorption versus entropy of adsorption at different moisture content calculated according to eq 9 is shown in Figure 14.

As can be seen from Figure 14, for both one-component and two-component injections, the adsorption entropy of CH_4/CO_2 generally decreases with the increase of moisture content, and the adsorption entropy of CO_2 < CH_4 decreases. According to the analysis of Figure 14, R^2 decreases from 0.97 to 0.68, which indicates that the correlation between the adsorption amount of CH_4/CO_2 and the adsorption entropy is gradually far from each other, and a new curvilinear relationship may exist. When the adsorption amount is the same, the adsorption entropy is CH_4 > CO_2. When the adsorption entropy value is the same, the adsorption amount is CH_4 < CO_2. At the moisture content of 10%, a large amount of

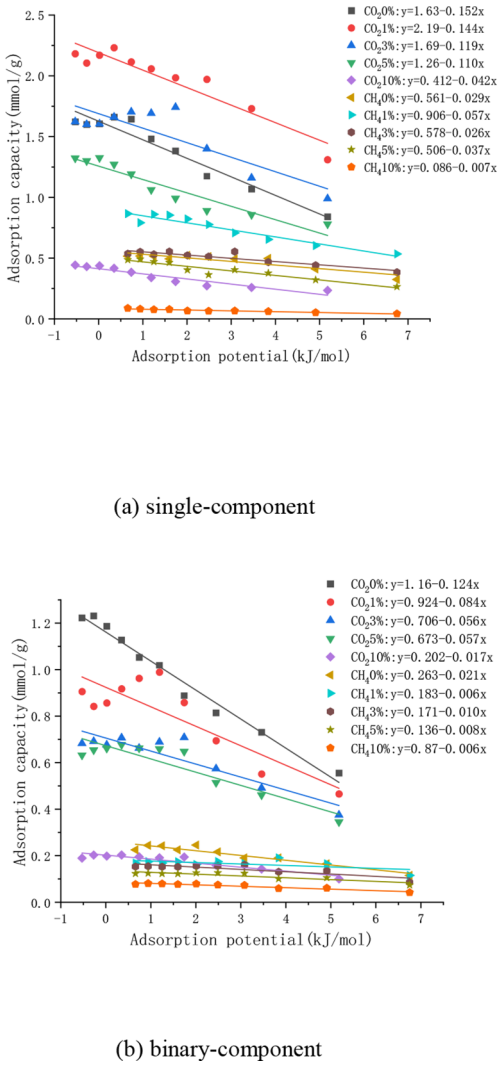

Figure 13. Adsorption potential energy versus adsorption capacity curves at different moisture content: (a) single-component and (b) binary-component.

H_2O is more orderly arranged, the interaction force between H_2O and the coal body is enhanced, and the H_2O occupies most of the adsorption sites. The above analysis shows that when the moisture content is less than 1%, H_2O will increase the adsorption sites, which is favorable for CO_2 to replace CH_4. When the moisture content is higher than 10%, a large amount of H_2O will compete for the adsorption sites of CH_4/CO_2, which significantly reduces the adsorption amount of CH_4/CO_2, which is unfavorable for CO_2 sequestration.

4. CONCLUSIONS

In this study, the adsorption isotherm, heat of adsorption, potential energy of adsorption, and entropy of adsorption of coal on CH_4/CO_2 were obtained by molecular simulations at different temperatures (298, 308, and 318 K), adsorption pressures (0−10 MPa), and moisture contents (0−10%). The following conclusions are drawn:

1. CH_4 molecules in coal macromolecules are distributed in a low-density dispersed state and CO_2 molecules are distributed in a high-density aggregated form in the pores of coal at different temperatures or moisture content. Temperature and moisture content are negatively correlated with the

https://doi.org/10.1021/acsomega.3c07872
ACS Omega 2023, 8, 48381−48393

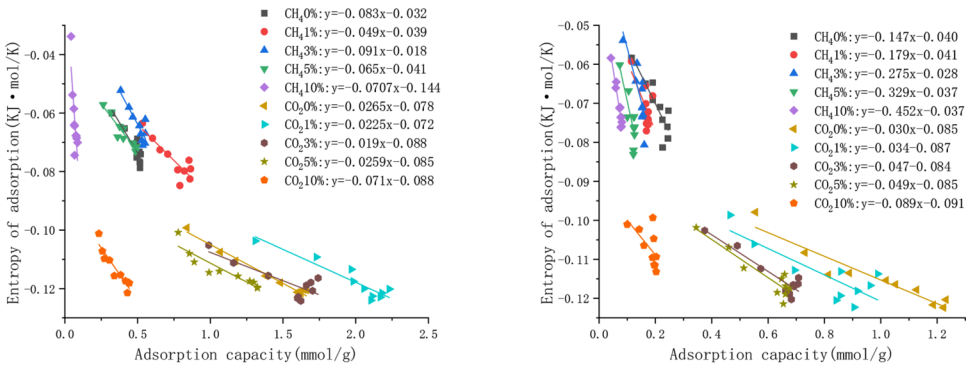

(a) single-component (b)binary-component

Figure 14. Adsorption versus entropy curves for different moisture content: (a) single-component and (b) binary-component.

adsorption constants a and b. At a fixed temperature or moisture content, CH_4/CO_2 adsorption increases with increasing pressure, but there is a saturation point of adsorption. As the temperature increases, the pressure required to reach the saturated adsorption capacity of the coal decreases.

2. Under the same conditions, the relationship of adsorption amount was CO_2 > CH_4 and the relationship of heat of adsorption was CO_2 > CH_4. Changes in the temperature and moisture content affected the equivalent heat of adsorption, while changes in the pressure had no significant effect. Temperature and moisture content were negatively correlated with the adsorption capacity of CH_4/CO_2. The potential energy of adsorption of CH_4/CO_2 was negatively correlated with the adsorption amount with increasing temperature, while it was positively correlated with the adsorption amount with increasing pressure. With the increase of the moisture content, the adsorption potential energy of CH_4/CO_2 will reach the peak at a moisture content of less than 1%, and the adsorption potential energy will decrease significantly when the moisture content is more than 10%.

3. At different temperatures, CH_4/CO_2 adsorption was negatively correlated with the entropy of adsorption, and as the temperature increased, the entropy of CH_4/CO_2 adsorption increased and more CH_4/CO_2 was in the free state. Therefore, at temperatures higher than 318 K, CH_4 is less likely to be controlled and CO_2 is less likely to be sequestered. The adsorption amount of CH_4/CO_2 decreased with the increase of moisture content at different moisture content. When the adsorption amount is the same, the adsorption entropy is CH_4 > CO_2. When the adsorption entropy value is the same, the adsorption amount is CH_4 < CO_2. In the moisture content of 1%, it is favorable for CO_2 to displace CH_4. In the moisture content of > 10%, although CO_2 adsorption is better than CH_4, a large amount of H_2O will occupy adsorption sites and form an aqueous film, and the H_2O has a large effect on CO_2.

4. The higher the system pressure of coal adsorption of CH_4/CO_2, the relatively larger the adsorption amount, but there is an adsorption pressure point of the saturation adsorption amount. When the temperature is higher than 318 K, the adsorption amount of CO_2 and CH_4 decreases significantly, which is unfavorable for CO_2 sequestration and CH_4 control. When the moisture content is less than 1%, it is favorable for CO_2 sequestration and CO_2 replacement of CH_4. When the water content is higher than 10%, H_2O occupies most of the adsorption points, and the adsorption amount of both CH_4 and CO_2 decreases significantly, which is unfavorable for CO_2 replacement of CH_4 and CO_2 sequestration.

However, there are shortcomings and limitations in the simulation conditions that we chose. Whether higher temperatures and water contents are consistent with the results of the study is something we need to study in depth given the complexity of CBM reservoir conditions. The next step is to select a wider range of temperatures and water contents or add other conditions to characterize the adsorption of coal on CH_4/CO_2, which we will do next.

AUTHOR INFORMATION

Corresponding Author

Xingyu Wu − *Institute of Mining and Coal, Inner Mongolia University of Science and Technology, Baotou 014010, China;* orcid.org/0009-0006-5413-1825; Email: 983767000@qq.com

Authors

Tinggui Jia − *Institute of Mining and Coal, Inner Mongolia University of Science and Technology, Baotou 014010, China*

Guona Qu − *Institute of Mining and Coal, Inner Mongolia University of Science and Technology, Baotou 014010, China*

Complete contact information is available at: https://pubs.acs.org/10.1021/acsomega.3c07872

Funding

This work is supported by the Inner Mongolia Autonomous Region Nature Fund Major Project (2022LHMS05019); the Inner Mongolia Autonomous Region Nature Fund Major Project (2022LHMS05020); and the Inner Mongolia Autonomous Region Higher Education Institutions Natural Science Key Project (NJZZ21025).

Notes

The authors declare no competing financial interest.

ACKNOWLEDGMENTS

The authors acknowledge the financial support from the Inner Mongolia Autonomous Region Nature Fund (grant numbers 2022LHMS05019 and 2022LHMS05020).

https://doi.org/10.1021/acsomega.3c07872
ACS Omega 2023, 8, 48381−48393

REFERENCES

(1) Sharma, R.; Singh, S.; Anand, S.; Kumar, R. A review of coal bed methane production techniques and prospects in India. *Mater. Today: Proc.* **2023**, DOI: 10.1016/j.matpr.2023.08.150.

(2) Rodrigues, C. F.; de Sousa, M. J. L. The measurement of coal porosity with different gases. *Int. J. Coal Geol.* **2002**, *48*, 245−251.

(3) Gensterblum, Y.; Merkel, A.; Busch, A.; Krooss, B. M. High-pressure CH_4 and CO_2 sorption isotherms as a function of coal maturity and the influence of moisture. *International Journal of Coal Geology* **2013**, *118*, 45−57.

(4) Moore, T. A. Coalbed methane: A review. *International Journal of Coal Geology* **2012**, *101*, 36−81.

(5) Jiang, L.; Chen, Z.; Farouq Ali, S. M.; Zhang, J.; Chen, Y.; Chen, S. Storing carbon dioxide in deep unmineable coal seams for centuries following underground coal gasification. *Journal of Cleaner Production* **2022**, *378*, No. 134565.

(6) Pan, Z.; Ye, J.; Zhou, F.; Tan, Y.; Connell, L. D.; Fan, J. CO_2 storage in coal to enhance coalbed methane recovery: a review of field experiments in China. *Int. Geol. Rev.* **2018**, *60*, 754−776.

(7) Wu, H.; Jin, Z.; Xu, X.; Zhao, S.; Liu, H. Effect of competitive adsorption on the deformation behavior of nanoslit-confined carbon dioxide and methane mixtures. *Chemical Engineering Journal* **2022**, *431*, No. 133963.

(8) Damen, K.; Faaij, A.; van Bergen, F.; Gale, J.; Lysen, E. Identification of early opportunities for CO_2 sequestration—worldwide screening for CO_2-EOR and CO_2-ECBM projects. *Energy* **2005**, *30*, 1931−1952.

(9) Liu, Z.; Feng, Z. Theoretical study on the heat of adsorption of coal body to gas. *J. Coal* **2012**, *37*, 647−653.

(10) Bachu, S.; Bonijoly, D.; Bradshaw, J.; Burruss, R.; Holloway, S.; Christensen, N. P.; et al. CO_2 storage capacity estimation: Methodology and gaps. *International Journal of Greenhouse Gas Control* **2007**, *1*, 430−443.

(11) Goodman, A. L.; Busch, A.; Bustin, R. M.; Chikatamarla, L.; Day, S.; Duffy, G. J.; et al. Inter-laboratory comparison II: CO_2 isotherms measured on moisture-equilibrated Argonne premium coals at 55 °C and up to 15 MPa. *International Journal of Coal Geology* **2007**, *72*, 153−164.

(12) Wang, L.; Wang, Z.; Li, K.; Chen, H. Comparison of enhanced coalbed methane recovery by pure N2 and CO_2 injection: Experimental observations and numerical simulation. *Journal of Natural Gas Science and Engineering* **2015**, *23*, 363−372.

(13) Ma, D.; Li, L.; Li, X. Comparison of CH_4 and CO_2 adsorption and desorption experiments of No. 4 coal from Dafosi well field. *J. Coal* **2014**, *39*, 8023.

(14) Krooss, B. M.; van Bergen, F.; Gensterblum, Y.; Siemons, N.; Pagnier, H. J. M.; David, P. High-pressure methane and carbon dioxide adsorption on dry and moisture-equilibrated Pennsylvanian coals. *International Journal of Coal Geology* **2002**, *51*, 69−92.

(15) Day, S.; Sakurovs, R.; Weir, S. Supercritical gas sorption on moist coals. *International Journal of Coal Geology* **2008**, *74*, 203−214.

(16) Zhou, F.; Hussain, F.; Cinar, Y. Injecting pure N2 and CO_2 to coal for enhanced coalbed methane: Experimental observations and numerical simulation. *International Journal of Coal Geology* **2013**, *116−117*, 53−62.

(17) Zhang, S.; Zhang, S.; Tang, S. Adsorption and transportation law of methane and carbon dioxide mixture in anthracite coal. *J. Coal* **2021**, *46* (2), 544−555.

(18) Lun, J. Gas adsorption characteristics of coal nanopore structure. *China Univ. Min. Technol.* **2020**, DOI: 10.27624/d.cnki.gzkbu.2020.000075.

(19) Wen, H.; Wang, H.; Fan, S.; Li, Z.; Chen, J.; Cheng, X.; et al. Improving coal seam permeability and displacing methane by injecting liquid CO_2: An experimental study. *Fuel* **2020**, *281*, No. 118747.

(20) Liu, S.; Fang, H.; Sang, S.; Ashutosh, T.; Wu, J.; Zhang, S.; et al. CO_2 injectability and CH_4 recovery of the engineering test in qinshui Basin, China based on numerical simulation. *International Journal of Greenhouse Gas Control* **2020**, *95*, No. 102980.

(21) Long, H.; Lin, H.; Yan, M.; Chang, P.; Li, S. g.; Bai, Y. Molecular simulation of the competitive adsorption characteristics of CH_4, CO_2, N_2, and multicomponent gases in coal. *Powder Technol.* **2021**, *385*, 348−356.

(22) Dang, Y.; Zhao, L.; Lu, X.; Xu, J.; Sang, P.; Guo, S.; et al. Molecular simulation of CO_2/CH_4 adsorption in brown coal: Effect of oxygen-, nitrogen-, and sulfur-containing functional groups. *Appl. Surf. Sci.* **2017**, *423*, 33−42.

(23) Qu, G.-n.; Ma, Z.-x.; Jia, T.-g.; Lou, H.-z.; Qiang, Q.; Hao, Y. Experimental and molecular simulation study of CH_4 and CO_2 gas adsorption by highly metamorphosed coal. *J. Safety Environ.* **2022**, *2022*, 142−147.

(24) Hua, X. J.; Zeng, F. G.; Liang, H. Z.; Li, B.; Song, X. X. Molecular simulation of the CH_4/CO_2/ H_2O adsorption onto the molecular structure of coal. *Science China (Earth Sciences)* **2014**, *57*, 1749−1759.

(25) Jia, J.; Wu, Y.; Zhao, D.; Li, B.; Wang, D.; Wang, F. Adsorption of CH_4/CO_2/N2 by different functional groups in coal. *Fuel* **2023**, *335*, No. 127062.

(26) Hao, M.; Wei, C.; Qiao, Z. Effect of internal moisture on CH_4 adsorption and diffusion of coal: A molecular simulation study. *Chem. Phys. Lett.* **2021**, *783*, No. 139086.

(27) Zhang, J.; Wei, C.; Zhao, C.; Zhang, T.; Lu, G.; Zou, M. Effects of nano-pore and macromolecule structure of coal samples on energy parameters variation during methane adsorption under different temperature and pressure. *Fuel* **2021**, *289*, No. 119804.

(28) Lou, H.; Jia, T. Differential study of competitive adsorption of inert atmosphere on the spontaneous combustion process of coal. *Chinese J. Safety Sci.* **2020**, *30*, 1.

(29) Zhang, X.; Cai, Y.; Zhou, T.; Cheng, J.; Zhao, G.; Zhang, L.; et al. Thermodynamic characteristics of methane adsorption on coals from China with selected metamorphism degrees: Considering the influence of temperature, moisture content, and in situ modification. *Fuel* **2023**, *342*, No. 127771.

(30) Gensterblum, Y.; Busch, A.; Krooss, B. M. Molecular concept and experimental evidence of competitive adsorption of H_2O, CO_2 and CH_4 on organic material. *Fuel* **2014**, *115*, 581−588.

(31) Abunowara, M.; Bustam, M. A.; Sufian, S.; Babar, M.; Eldemerdash, U.; Mukhtar, A.; et al. High pressure CO_2 adsorption onto Malaysian Mukah-Balingian coals: Adsorption isotherms, thermodynamic and kinetic investigations. *Environmental Research* **2023**, *218*, No. 114905.

(32) Busch, A.; Gensterblum, Y. CBM and CO_2-ECBM related sorption processes in coal: A review. *International Journal of Coal Geology* **2011**, *87*, 49−71.

(33) Li, Z.; Bai, Y.; Yu, H.; Hu, H.; Wang, Y. Molecular simulation of thermodynamic properties of CH_4 and CO_2 adsorption under different moisture content and pore size conditions. *Fuel* **2023**, *344*, No. 127833.

(34) Chai, Z.; Zeng, Q. Construction and characterization of molecular structure model of coal from Wucaiwan in Jundong based on quantum chemistry. *J. Coal Sci.* **2022**, *47* (12), 4504−4516.

(35) Liu, X.; Ma, J.; Xu, J. Study on the effect of moisture on methane adsorption characteristics of soft and hard anthracite coal based on molecular simulation method. *Coal Mine Safety* **2022**, *53*, 20−27.

(36) Garnier, Ch; Finqueneisel, G.; Zimny, T.; Pokryszka, Z.; Lafortune, S.; Défossez, P. D. C.; et al. Selection of coals of different maturities for CO_2 Storage by modelling of CH_4 and CO_2 adsorption isotherms. *International Journal of Coal Geology* **2011**, *87*, 80−86.

(37) Yan, M.; Bai, Y.; Li, S.-G.; Lin, H.-F.; Yan, D.-J.; Shu, C.-M. Factors influencing the gas adsorption thermodynamic characteristics of low-rank coal. *Fuel* **2019**, *248*, 117−126.

(38) Tang, X.; Wang, Z.; Ripepi, N.; Kang, B.; Yue, G. Adsorption Affinity of Different Types of Coal: Mean Isosteric Heat of Adsorption. *Energy Fuels* **2015**, *29*, 3609−3615.

(39) Lin, H.; Long, H.; Yan, M.; Li, S.; Shu, C.-M.; Bai, Y. Methane adsorption thermodynamics of coal sample subjected to liquid

https://doi.org/10.1021/acsomega.3c07872
ACS Omega 2023, 8, 48381−48393

nitrogen freezing−thawing process. *Journal of Natural Gas Science and Engineering* **2021**, *90*, No. 103896.
(40) Magomedov, M. N. On the accuracy of the Clausius-Clapeyron relation. *Vacuum* **2023**, *217*, No. 112494.
(41) Polanyi, M. The potential theory of adsorption. *Science* **1963**, *141* (3585), 1010−1013.
(42) Mathias, P. M.; O'Connell, J. P. The Gibbs−Helmholtz Equation and the Thermodynamic Consistency of Chemical Absorption Data. *Ind. Eng. Chem. Res.* **2012**, *51*, 5090−5097.
(43) Monsalvo, M. A.; Shapiro, A. A. Study of high-pressure adsorption from supercritical fluids by the potential theory. *Fluid Phase Equilib.* **2009**, *283*, 56−64.
(44) Dubinin, M. M. The Potential Theory of Adsorption of Gases and Vapors for Adsorbents with Energetically Nonuniform Surfaces. *Chem. Rev.* **1960**, *60*, 235−241.
(45) Wen, H.; Tangrui, L. M. Molecular simulation study of C_2H_4 adsorption in bituminous coal. *Coal Mine Safety* **2023**, 54.
(46) Sun, Y.; Wang, L.; Wang, R.; Zheng, S.; Liao, X.; Zhu, Z.; et al. Insight on microscopic mechanisms of CH_4 and CO_2 adsorption of coal with different ranks. *Fuel* **2022**, *330*, No. 125715.
(47) Du, C.; Nasajpour-Esfahani, N.; Hekmatifar, M.; Toghraie, D.; Esmaeili, S. The effect of initial temperature and external heat flux on the H_2 and CO production by biomass gasification using molecular dynamics simulation. *Renewable Energy* **2023**, *215*, No. 119011.
(48) Zhou, J.; Tian, S.; Yang, K.; Dong, Z.; Cai, J. Chapter Eleven - Enhanced gas recovery technologies aimed at exploiting captured carbon dioxide. In *Sustainable Natural Gas Reservoir and Production Engineering*, Wood, D. A.; Cai, J., Eds.; vol *1*, Gulf Professional Publishing; 2022; p 305−347.
(49) Du, X.; Cheng, Y.; Liu, Z.; Yin, H.; Wu, T.; Huo, L.; et al. CO_2 and CH_4 adsorption on different rank coals: A thermodynamics study of surface potential, Gibbs free energy change and entropy loss. *Fuel* **2021**, *283*, No. 118886.
(50) Qin, Y.; Su, W.; Tian, F.; Chen, Y. Current status and development direction of research on microscopic effects of coal bed water injection. *J. China Univ. Min. Technol.* **2020**, *49*, 428−444.
(51) Xi, Z.; Li, X.; Xi, K. Study on the reactivity of oxygen-containing functional groups in coal with and without adsorbed water in low-temperature oxidation. *Fuel* **2021**, *304*, No. 121454.
(52) Zhao, J.; Deng, S.; Zhao, L.; Yuan, X.; Wang, B.; Chen, L.; et al. Synergistic and competitive effect of H_2O on CO_2 adsorption capture: Mechanism explanations based on molecular dynamic simulation. *Journal of CO2 Utilization* **2021**, *52*, No. 101662.

https://doi.org/10.1021/acsomega.3c07872
ACS Omega 2023, 8, 48381−48393